Implementation and Performance of the High Level Trigger Electron and Photon Selection for the ATLAS Experiment at the LHC

Carlo Schiavi on behalf of the ATLAS High Level Trigger Group* [1]

***Abstract*— The ATLAS experiment at the Large Hadron Collider (LHC) will face the challenge of efficiently selecting interesting candidate events in pp collisions at 14 TeV center of mass energy, while rejecting the enormous number of background events, stemming from an interaction rate of up to 10^9 Hz. The First Level trigger will reduce this rate to around $\mathcal{O}$(100 kHz). Subsequently, the High Level Trigger (HLT), which is comprised of the Second Level trigger and the Event Filter, will need to further reduce this rate by a factor of $\mathcal{O}(10^3)$. The HLT selection is software based and will be implemented on commercial CPUs, using a common framework built on the standard ATLAS object oriented software architecture. In this paper an overview of the current implementation of the selection for electrons and photons in the HLT is given. The performance of this implementation has been evaluated using Monte Carlo simulations in terms of the efficiency for the signal channels, rate expected for the selection, data preparation times, and algorithm execution times. Besides the efficiency and rate estimates, some physics examples will be discussed, showing that the triggers are well adapted for the physics programme envisaged at LHC. The electron and photon trigger software is also being exercised at the ATLAS 2004 Combined Test Beam, where components from all ATLAS subdetectors are taking data together along the H8 SPS extraction line; from these tests a validation of the selection architecture chosen in a real on-line environment is expected.**

***Index Terms*— ATLAS, Trigger, Electron, Photon, Higgs**

* S. Armstrong[a], A. dos Anjos[b], J. T. M. Baines[c], C. P. Bee[d], , M. Biglietti[e], J. A. Bogaerts[f], V. Boisvert[f], M. Bosman[g], B. Caron[h], P. Casado[g], G. Cataldi[i], D. Cavalli[j], M. Cervetto[k], G. Comune[l], P. Conde Muino[f], A. De Santo[m], M. Diaz Gomez[n], M. Dosil[g], N. Ellis[f], D. Emeliyanov[c], B. Epp[o], S. Falciano[p], A. Farilla[q], S. George[m], V. Ghete[o], S. Gonzalez[r], M. Grothe[f], S. Kabana[l], A. Khomich[s], G. Kilvington[m], N. Konstantinidis[t], A. Kootz[u], A. Lowe[m], L. Luminari[p], T. Maeno[f], J. Masik[v], A. Di Mattia[p], C. Meessen[d], A. G. Mello[b], G. Merino[g], R. Moore[h], P. Morettini[k], A. Negri[w], N. Nikitin[x], A. Nisati[p], C. Padilla[f], N. Panikashvili[y], F. Parodi[k], V. Perez Reale[l], J. L. Pinfold[h], P. Pinto[f], Z. Qian[d], S. Resconi[j], S. Rosati[f], C. Sanchez[g], C. Santamarina[f], D. A. Scannicchio[w], C. Schiavi[k], E. Segura[g], J. M. de Seixas[b], S. Sivoklokov[x], R. Soluk[h], E. Stefanidis[t], S. Sushkov[g], M. Sutton[t], S. Tapprogge[z], E. Thomas[l], F. Touchard[d], B. Venda Pinto[aa], V. Vercesi[w], P. Werner[f], S. Wheeler[h,bb], F. J. Wickens[c], W. Wiedenmann[r], M. Wielers[cc], G. Zobernig[r]

[a]Brookhaven National Laboratory (BNL), Upton, New York, USA. [b]Universidade Federal do Rio de Janeiro, COPPE/EE, Rio de Janeiro, Brazil. [c]Rutherford Appleton Laboratory, Chilton, Didcot, UK. [d]Centre de Physique des Particules de Marseille, IN2P3-CNRS-Université d'Aix-Marseille 2, France [e]University of Michigan, Ann Arbor, Michigan, USA. [f]CERN, Geneva, Switzerland. [g]Institut de Física d'Altes Energies (IFAE), Universidad Autónoma de Barcelona, Barcelona, Spain. [h]University of Alberta, Edmonton, Canada. [i]Dipartimento di Fisica dell'Università di Lecce e I.N.F.N., Lecce, Italy. [j]Dipartimento di Fisica dell'Università di Milano e I.N.F.N., Milan, Italy. [k]Dipartimento di Fisica dell'Università di Genova e I.N.F.N., Genova, Italy. [l]Laboratory for High Energy Physics, University of Bern, Switzerland. [m]Department of Physics, Royal Holloway, University of London, Egham, UK. [n]Section de Physique, Université de Genève, Switzerland. [o]Institut für Experimentalphysik der Leopald-Franzens Universität, Innsbruck, Austria. [p]Dipartimento di Fisica dell'Università di Roma "La Sapienza" e I.N.F.N., Rome, Italy. [q]Dipartimento di Fisica dell'Università di Roma "Roma Tre" e I.N.F.N., Rome, Italy. [r]Department of Physics, University of Wisconsin, Madison, Wisconsin, USA. [s]Lehrstuhl für Informatik V, Universität Mannheim, Mannheim, Germany. [t]Department of Physics and Astronomy, University College London, London, UK. [u]Fachbereich Physik, Bergische Universitat Wuppertal, Germany. [v]Institute of Physics, Academy of Sciences of the Czech Republic, Prague, Czech Republic. [w]Dipartimento di Fisica Nucleare e Teorica dell'Università di Pavia e INFN, Pavia, Italy. [x]Institute of Nuclear Physics, Moscow State University, Moscow, Russia. [y]Department of Physics, Technion, Haifa, Israel. [z]Institut für Physik, Universität Mainz, Mainz, Germany. [aa]CFNUL - Universidade de Lisboa, Faculdade de Ciências, Lisbon, Portugal.[bb]University of California at Irvine, Irvine, USA. [cc]University of Victoria, Victoria, Canada.

I. Introduction

THE ATLAS (A Toroidal LHC ApparatuS) experiment will start taking data in 2007 at the Large Hadron Collider (LHC), a pp collider, which is currently under construction at the European Organization for Nuclear Research (CERN). At the LHC, protons will collide at a centre of mass energy of $14\,\mathrm{TeV}$, with a bunch spacing of $25\,\mathrm{ns}$ and a design luminosity of $10^{34}\,\mathrm{cm}^{-2}\,\mathrm{s}^{-1}$.

ATLAS [2] is a multipurpose experiment, designed to cover various aspects of high energy physics phenomenology: discovering new physical phenomena, like Higgs bosons or supersymmetrical particles, predicted by theories compatible with the current experimental observations; performing precision Standard Model (SM) studies, like measurements of the t quark and W boson masses; detecting possible unexpected signals from unpredicted physics scenarios. To achieve this goal, moving from the inside out, the ATLAS detector is equipped as follows: tracking and particle identification detectors (Pixel, SCT silicon strips and TRT straw tubes), forming the so called Inner Detector (ID) [3]; Liquid Argon (LAr) electromagnetic and Tile and LAr hadronic calorimeters [4]; outer muon system [5], designed both for tracking (Monitored Drift Tubes and Cathode Strip Chambers) and trigger purposes (Resistive Plate and Thin Gap Chambers).

At design luminosity, $\sim$ 23 pp interaction will occur at every bunch crossing, in addition to any interesting physics events; together with the bunch spacing of $25\,\mathrm{ns}$, this poses stringent design demands on both the detectors and the Trigger and Data Acquisition (TDAQ) system [6].

From the hardware side, this means, as an example, that every subdetector must be equipped with built-in pipeline memories,

to temporarily store events while the first level trigger decision is taken; furthermore the entire detector, which is $22\,\mathrm{m}$ tall and $44\,\mathrm{m}$ long, must be synchronized to better than $25\,\mathrm{ns}$, in order to ensure a correct event building. On the other side, the high number of detector channels, $\mathcal{O}(10^8)$ in total, leads to a mean event size of $\sim 1.5\,\mathrm{MB}$; this means that the TDAQ has to face a very challenging networking task, while at the same time has to limit the final event storage rate to a maximum value of $\sim 200\,\mathrm{Hz}$. This last requirement must be fulfilled through the event rejection performed by the trigger system.

II. The ATLAS trigger system

In the beginning of this section, the general ATLAS trigger scheme is described; subsequently more detail is given to the High Level Trigger (HLT) strategy and implementation.

A. General trigger scheme

In the ATLAS experiment, reduction of the $1\,\mathrm{GHz}$ interaction rate down to the $200\,\mathrm{Hz}$ maximum event data storage rate will be provided through three different trigger selection layers, as shown in figure 1.

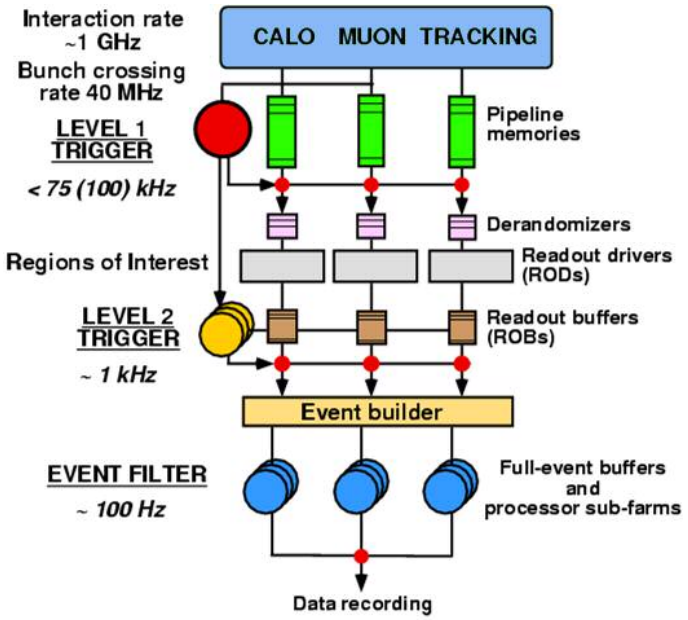

Fig. 1. Block diagram of the ATLAS Trigger/DAQ system.

The hardware-based First Level trigger (LVL1) performs a preliminary rejection using only reduced granularity data coming from the calorimeters and the muon detectors; it operates within a $2\,\mu\mathrm{s}$ latency, producing an average output rate of $75\,\mathrm{kHz}$, upper limited to $100\,\mathrm{kHz}$.
Further event selection is then performed by software tools running on dedicated commercial processor farms and is divided in two layers, the Second Level trigger (LVL2) and the Event Filter (EF), collectively referenced as HLT. The choice of having two different software selection levels, though increasing the complexity of the system, has the effect of significantly reducing the computing power needs and of improving the flexibility of the event selection scheme.
Reconstruction at LVL2, seeded by information collected at LVL1, can exploit full granularity information from all ATLAS subdetectors; it is performed processing in parallel data contained inside one or more geometrical regions identified at LVL1, the so called Regions of Interest (RoI), each corresponding on average to the 2% of the total event.
Event selection is designed in order to provide an output rate below $2\,\mathrm{kHz}$, and the LVL2 decision must be taken with a mean processing time of $10\,\mathrm{ms}$; obviously the limited execution time greatly contraints the LVL2 reconstruction algorithms, which have to be optimized for timing performance and whose complexity is strongly constrained.
The EF has much looser time constraints of the order of $1\,\mathrm{s}$. It can in its turn be seeded by the LVL2 results, or the whole event can be analysed, as an example for the missing transverse energy triggers. More complex reconstruction strategies, including bremsstrahlung and converted photon recovery, can be adopted at this stage.

B. The HLT event selection

The main two concepts characterizing event selection at the HLT in the ATLAS experiment are the RoI-guided reconstruction and the step processing steering.
The Region of Interest (RoI) mechanism is used, mainly at LVL2, to significantly reduce the amount of data to be analyzed, and thus processing time, while retaining the full rejection power of a software selection based on full granularity data from all the detectors.
All the information gathered at LVL1, like the geometrical position in η and ϕ of the tagged objects and the thresholds they passed, are combined into a single RoI record which is then sent to the LVL2 framework.
As described in more detail in the next subsections, only data produced by detector modules inside the LVL1 RoI will be asked to the Data Flow software (DF), which takes care of all data movement needs from data acquisition to the final storage, and passed to the LVL2; this way a lot of network bandwidth and processing time can be saved.
Another feature peculiar to the ATLAS HLT event selection strategy is the early rejection, achieved through event processing in alternate steps of event reconstruction and hypothesis testing on the reconstructed quantities [9]; this means that an event can be rejected after any of these steps, if the reconstructed features do not fulfil required criteria or signatures. This method proves particularly powerful at LVL2, where the different RoIs are processed in parallel; as a matter of fact if a minimum number of RoIs is required to pass the selection cuts in order to accept the event, as soon as too many RoIs are prematurely rejected and the minimum required number cannot be met, all the parallel reconstruction tasks taking care of each RoI are stopped and the whole event is rejected.

C. The HLT data access scheme

The goal of minimizing the processing time and network transfers during HLT operation is also pursued through the data access scheme adopted, shown in figure 3.

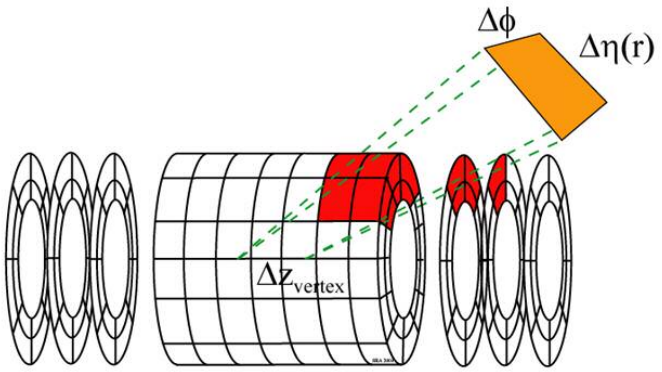

Fig. 2. The Region Selector tool: each geometrical (η, ϕ) region is converted into a set of detector elements to be analyzed by LVL2 algorithms.

Every time an HLT algorithm is seeded by a RoI, the corresponding geometrical information is passed to the Region Selector service in order to be transformed into a list of detector elements contained inside the RoI, as depicted in figure 2; addressing of detector elements, corresponding to subdetector

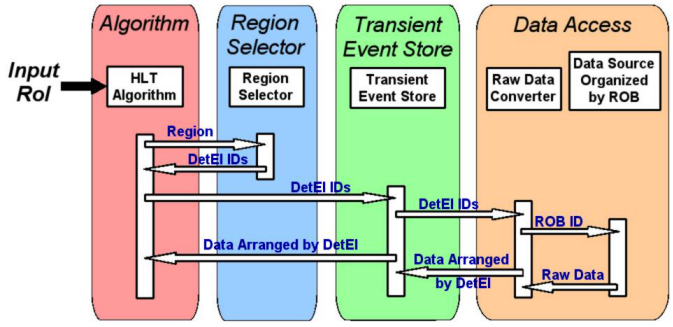

Fig. 3. HLT algorithm data access scheme.

modules or read-out channels, is univocally performed using the so called detector element identifiers. To optimize the timing performance, the mapping of the geometrical (η, ϕ) region into the unique identifiers for the readout units and their corresponding detector elements is implemented using fast look-up tables.

The list of identifiers received from the Region Selector is then passed to the Transient Event Store and then to the Data Access tools which request data to the DF software only for the Read-out Buffers (RoB) containing the required detector elements. During this stage, raw data also undergoes the conversion from binary read-out channel information to higher level objects containing more physical and algorithm-oriented data, such as calorimeter cell information or ID space points.

Decoded data, ordered by detector element, is then passed back to the Transient Event Store [8], a service also used by the offline reconstruction, and eventually to the algorithm that issued the request; transient data is also temporarily cached to avoid another access to the DF and another decoding process in case it will be reasked, as an example by another HLT algorithm.

III. Electron and photon selection

In this section the physical importance of an effective electron and photon selection is discussed along with their signatures, with particular emphasis on the ATLAS HLT implementation.

A. Physical relevance of electron and photon signatures

Many interesting physical phenomena at LHC, such as $H \rightarrow 4e$, lead to a final state containing isolated electrons and/or photons, which provide very clean signatures; they are therefore very important in the reconstruction of possible discovery channels with a high statistical significance. Moreover, electron selection will prove very valuable also for detector calibration and alignment and during the commissioning phase; as an example, a common channel like $Z \rightarrow ee$ is a multipurpose tool with many key applications.

Electron and photon reconstruction mainly exploits data coming from the EM LAr calorimeter and the ID tracking systems; this way not only the kinematical properties of these particles are obtained, taking into account bremsstrahlung effects and photon conversions, but also significant particle identification and rejection of fake e/γ candidates can be achieved, which proves essential for online event selection, as described in detail in the next subsection.

B. Implementation at the HLT

The procedure for the electron and photon selection at the HLT is guided by the Region of Interest mechanism.

In particular, LVL2 reconstruction uses information on the transverse energy and the direction of the electromagnetic clusters selected by the LVL1 trigger, so that typically around 2% of the whole event needs to be further analysed. First the energy and position measurements obtained at LVL1 are refined; the leakage into the hadronic calorimeter is evaluated and variables related to the shower shape in the electromagnetic calorimeter are used to perform preliminary particle identification.

If a candidate is found to be consistent with an electron, track reconstruction is performed in the ID; cluster to track association is done using (η, ϕ) matching criteria, achieving further rejection against fake candidates; in case the matching was successful, the E_T/p_T ratio between the transverse energy measured in the EM calorimeter and the transverse momentum of the corresponding ID track is evaluated for particle identification.

In the case of photon candidates, reconstructed EM clusters undergo tighter shower shape cuts.

If the objects under analysis fulfil the required signatures, the event and its LVL2 result are passed to the EF, where

Trigger Step	Rate (Hz)	Efficiency (%)
LVL2 Calo	1.948 ± 46	95.6 ± 0.3
LVL2 Tracking	364 ± 21	89.4 ± 0.5
LVL2 Matching	143 ± 12	87.7 ± 0.6
EF Calo	101 ± 15	86.1 ± 0.6
EF Tracking	71 ± 10	82.0 ± 0.6
EF Matching	34 ± 6	79.7 ± 0.7

TABLE I

PERFORMANCE OF THE SINGLE ISOLATED ELECTRON HLT TRIGGER AT INITIAL LUMINOSITY.

Trigger Item	Luminosity	$H \to 4e$ (%)	$H \to \gamma\gamma$ (%)
$e25i$	*initial*	96.5 ± 0.2	
$2e15i$	*initial*	95.8 ± 0.2	
$e25$ or $2e15i$	*initial*	96.7 ± 0.2	
$e30i$	*design*	96.0 ± 0.4	
$2e20i$	*design*	94.5 ± 0.4	
$e30$ or $2e20i$	*design*	95.5 ± 0.3	
$2\gamma20i$	*initial*		74.0 ± 0.6
$\gamma60i$ or $2\gamma20i$	*initial*		83.0 ± 0.5

TABLE II

TRIGGER EFFICIENCIES FOR THE $H(130\,\mathrm{GeV}) \to 4e$ AND $H(120\,\mathrm{GeV}) \to \gamma\gamma$ CHANNELS AT INITIAL AND DESIGN LUMINOSITY.

information on the complete event is available, along with more precise calibrations and alignment constants. Even if selection at the EF follows the same scheme described for LVL2 operation, the looser timing constraints enable to employ more sophisticated reconstruction algorithms, taking care of bremsstrahlung recovery for electrons and conversion reconstruction for photons.

IV. RESULTS

In this section the performance of the HLT e/γ selection on both single trigger menus and their application to interesting physical channels is reported. Then preliminary results on timing are shown and the perspectives for testing the electron and photon selection on real data are described.

A. Single trigger menu studies

The performance of the e/γ trigger menus has been evaluated on Monte Carlo simulated samples for which the detector response has been simulated in detail; results are given in terms of the efficiency for the real electron and photon signals and of the expected output rates, directly related to the rejection power for fake candidates.

Table I shows the efficiency and expected rate for the trigger menu selecting single isolated electrons with a transverse energy (E_T) exceeding $25\,\mathrm{GeV}$ ($e25i$) at initial luminosity ($\mathcal{L} = 2 \times 10^{33}\,\mathrm{cm}^{-2}\,\mathrm{s}^{-1}$); errors, as also in the following, only take into account the statistical uncertainty contribution, while it should be noted that the uncertainties in the QCD di-jet cross-sections at the LHC are of the order of 2-3. Results have been evaluated on a simulated sample containing single electrons with $p_T = 25\,\mathrm{GeV}$ over the full tracking rapidity range $|\eta| < 2.5$. The efficiencies and rates are evaluated, after each HLT selection step, with respect to a LVL1 output efficiency of 95% and a LVL1 EM cluster rate of $12\,\mathrm{kHz}$, which are preliminary values.

Results show that a final electron selection efficiency of 80% with respect to LVL1 can be achieved with a final rate around $35\,\mathrm{Hz}$. The final selected sample mainly contains real electrons (44% from electrons from b and c quark decays, 21% from converted photons, 19% from $W \to e\nu$ decays, 1% from $Z \to ee$ decays). Only 25% of the rate is coming from fake clusters.

B. Application to physical channels

The aim of any trigger system is to provide the necessary event rate reduction, while preserving as much as possible the selection efficiency for interesting physical channels; a constant crosscheck on fully simulated events has hence to be performed, to ensure this goal is correctly met. In particular, for the HLT e/γ selection, studies have been performed on important physics channels such as $H \to 4e$ and $H \to \gamma\gamma$ (whose combination is crucial for Higgs discovery in the low mass region $100\,\mathrm{GeV} < m_H < 150\,\mathrm{GeV}$), $Z \to ee$ and $W \to e\nu$.

Table II shows the selection efficiencies for two samples of fully simulated Monte Carlo $H \to 4e$ and $H \to \gamma\gamma$ events. In this case, the efficiency is defined as the ratio of the final number of events selected by each trigger menu with respect to an initial sample, preselected according to geometrical and kinematical criteria, as used by the offline analyses [2], [10]. In particular, both electrons and photons must lay in the $|\eta| < 2.45$ region, but outside the barrel-endcap transition region $1.37 < |\eta| < 1.52$.

The final efficiencies obtained for each trigger configuration demonstrate that the trigger menus for electrons and photons are well adapted for the Higgs search programme envisaged at LHC.

C. Timing performance

As said before, timing performance is one of the most crucial issues related to HLT selection and reconstruction algorithms, especially at LVL2, and has thus to be continuously optimized to meet the design target.

As an example, here are reported the results obtained from a study on the execution times per RoI for LVL2 calorimeter cluster reconstruction; these also include the corresponding data preparation, which means the raw data accesses and the preprocessing needed by the HLT algorithms; all the estimations refer to execution on a LVL2 dedicated test-bed in a farm of $2.2\,\mathrm{GHz}$ processors and are performed operating inside $\Delta\eta \times \Delta\phi = 0.2 \times 0.2$ RoIs.

Figures 4 and 5 show the main contributions to the total latency for a sample of di-jet events at initial luminosity.

On figure 4 the total latency is reported and the dotted curve, corresponding to the integral of the distribution, shows that 95%

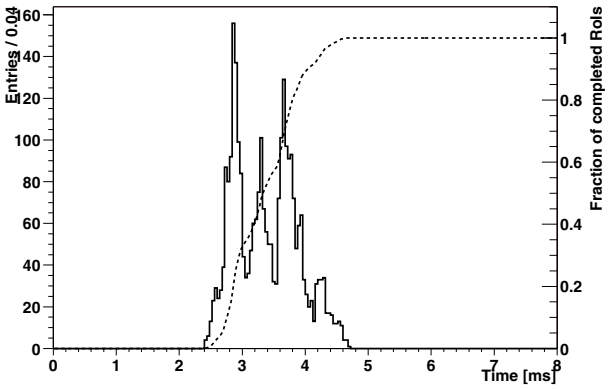

Fig. 4. EM calorimeter clustering: total execution time for LVL2 RoI processing of di-jet events at inital luminosity; results obtained on a 2.2 GHz processor.

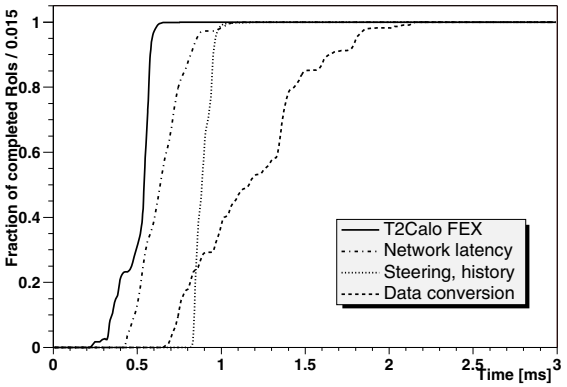

Fig. 5. EM calorimeter clustering: individual contributions to the execution time for LVL2 RoI processing of di-jet events at inital luminosity; results obtained on a 2.2 GHz processor.

of the events are processed within $5\,\mathrm{ms}$.

The four main contributions to the total latency are then shown, again as integrals of distributions, on figure 5. In order of decreasing importance we find data preparation and conversion, framework overheads, network access time, and algorithmic processing; results range between the $500\mu\mathrm{s}$ pure algorithm execution and the $1.8\,\mathrm{ms}$ within which data access is completed for 95% of the events.

Timing measurements for LVL2 tracking using the Pixel and SCT detectors have also been performed; the results hereafter reported have been obtained on initial luminosity single electron data sets and again refer to the reconstruction within a $\Delta\eta \times \Delta\phi = 0.2 \times 0.2$ RoI. This time the measurement was made using a machine equipped with a $2.8\,\mathrm{GHz}$ processor.

The results obtained for a LVL2 Silicon tracking algorithm are shown in figure 6, and refer to the algorithmic part only, excluding data access and preparation; they show that the mean execution time is around $560\mu\mathrm{s}$, and track reconstruction is completed within $1\,\mathrm{ms}$ in 95% of the events.

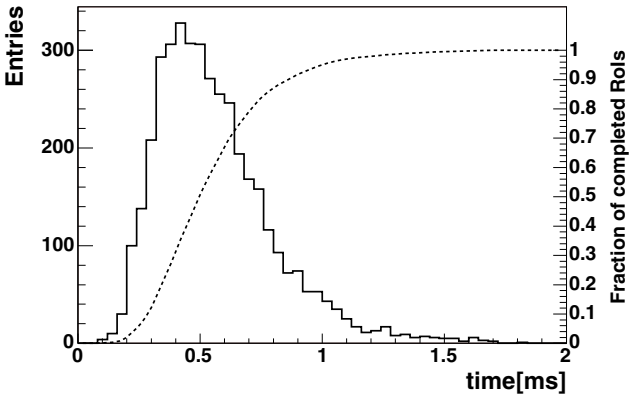

Fig. 6. Inner Detector tracking: total algorithmic execution time for LVL2 single electron reconstruction at inital luminosity; tracking is performed using data from the Pixel and SCT detectors within a $\Delta\eta \times \Delta\phi = 0.2 \times 0.2$ RoI; results obtained on a $2.8\,\mathrm{GHz}$ processor.

Continuous effort is put in improving all these timings, even if they are already well within the $10\,\mathrm{ms}$ target mean LVL2 decision time, in order to be sure that the same will hold once all the selection components will be exercised as a full chain; these results are even more encouraging if we imagine to scale them with a factor taking into account the improved computing power that will be available at startup, granted by the usage of $8\,\mathrm{GHz}$ processor farms.

D. Tests with real data

An important step towards the real operation during the experiment commissioning phase is the validation of the ATLAS TDAQ infrastructure in real or reconstructed online envionments.

Many activities on specific test-beds have already been performed and are still ongoing, and a good chance of testing the whole data taking and trigger chains on real online data is provided by the ATLAS Combined Test Beam (CTB) activity carried on this year at the H8 SPS extraction line at CERN.

Components from all ATLAS subdetectors (among which the ID and the EM LAr calorimeter, crucial for electron and photon selection) are aligned along the beam line and are currently taking data together; the geometry and the distance between subdetectors are designed to emulate a slice of the real ATLAS barrel detector. Figure 7 shows, an event taken at the CTB and, in particular, the hits produced by particles in the ID subdetectors.

From the computing point of view, data acquisition, event selection and reconstruction are based on the official ATLAS software, that will evolve in the final software for the experiment.

Among the goals of the ATLAS HLT community was to have an entire e/γ selection slice working at the Combined Test Beam. Online operation tests were performed both for the algorithms used in this slice (like the LVL2 track reconstruction and EF calorimeter clustering ones), for the e/γ hypothesis testing

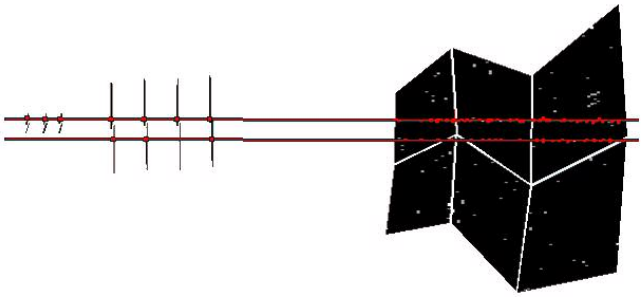

Fig. 7. Example of tracks reconstructed at the CTB from the hits produced by the corresponding particle in the ID subdetectors: from the left to the right are visible the three pixel layer, the four SCT layers and the TRT.

algorithm and for infrastructural components (e.g. testing the propagation of LVL2 resuts to the EF); an online monitoring histogram produced by the EF calorimeter cluster reconstruction algorithm is shown in figure 8.

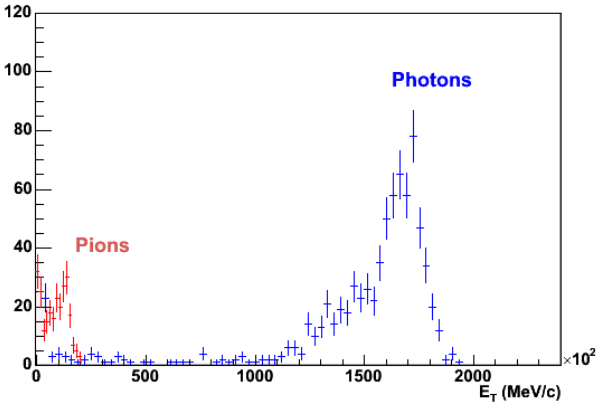

Fig. 8. EF calorimeter clustering: monitoring histogram for the transverse energy measurement performed through cluster reconstruction in the EM LAr calorimeter; distributions are compared for a photon and a pion run.

Although running the algorithms directly at the CTB provides interesting feedback on the TDAQ infrastructure, accurate HLT algorithms characterization will have to be done offline, where precise detector alignment and calibration will be available, enabling to correctly tune the algorithms. In particular it will be possible to study the results from runs with different particle composition: electrons, pions, muons and photons.
Furthermore, comparing HLT reconstruction with the offline one, many studies on algorithm and selection performance will be achievable: efficiency studies for both the detectors and the reconstruction; particle identification studies, using data from single detectors, in particular the TRT and the EM calorimeter, or from combined E_T/p_T evaluation; track to cluster (η, ϕ) matching; effects of bremsstrahlung on tracking and tests of the possible EF correction; studies on photon conversions.

V. Conclusion

The LHC environment poses challenging design issues to both the detectors and the TDAQ infrastructure.

As far as the trigger system is concerned, the ATLAS collaboration has adopted a three level strategy, in order to reduce the initial interaction rate of 10^9 Hz to a final event storage rate of about 200 Hz. The choice of having two software selection layers, altough leading to a more complex design, significantly reduces the needs for processing power and network bandwith and, at the same time, increases the flexibility of the selection strategies.
The goal of reducing computing power and networking needs is also evident in the HLT choice of using the RoI concept and the corresponding data access scheme, where only a few percentage of event data needs to be transfered and processed.
An effective selection of electrons and photons at the HLT is crucial, since they are involved as final signatures in many new physics phenomena expected at the LHC energies. Using Monte Carlo data sets for which the detector response was simulated in detail, the performance of the electron and photon trigger menus has been evaluated in terms of their selection efficiency and rate, and of timing performance both for the data preparation and the algorithmic processing. The preliminary results obtained look promising and in agreement with physics and technical design requirements.
In order to crosscheck the correct tuning of the e/γ trigger configuration, studies have been performed on the selection of important physics channels such as $H \rightarrow 4e$ or $H \rightarrow \gamma\gamma$. The results show that the current trigger menus for electrons and photons are correctly set-up to ensure the envisaged ATLAS physics programme.

References

[1] ATLAS HLT group, http://atlas.web.cern.ch/Atlas/GROUPS/DAQTRIG/HLT/AUTHORLISTS/nss2004.pdf
[2] ATLAS Collaboration, *ATLAS Detector and Physics Performance Technical Design Report*, CERN/LHCC/99-14, ATLAS-TDR-014 (1999).
[3] ATLAS Inner Detector Community, *Inner Detector Technical Design Report*, CERN/LHCC/97-16, ATLAS-TDR-4 (1997).
[4] ATLAS Collaboration, *Calorimeter Performance Technical Design Report*, CERN/LHCC/96-40 (1996).
[5] ATLAS Muon Collaboration, *ATLAS Muon Spectrometer Technical Design Report*, CERN/LHCC/97-22 (1997).
[6] ATLAS HLT/DAQ/DCS Group, *ATLAS High-Level Trigger, Data Acquisition and Controls Technical Design Report*, CERN/LHCC/2003-022, ATLAS-TDR-016 (2003).
[7] S. Armstrong et al., *An Implementation of Region-of-Interest Selection for ATLAS High Level Trigger and Offline Software Environments*, ATLAS Internal Note, ATL-DAQ-2003-014 (2003)
[8] P. Calafiura, C. Leggett, D.R. Quarrie, H. Ma, S. Rajagopalan, *The StoreGate: a Data Model for the Atlas Software Architecture*, ATLAS Internal Note, ATL-SOFT-2003-009, Proceedings CHEP03, La Jolla, California, March 24-28, 2003.
[9] G. Comune et al, *The Algorithm Steering and Trigger Decision mechanism of the ATLAS High Level Trigger*, ATLAS Internal Note, ATL-DAQ-2003-031, Proceedings CHEP03, La Jolla, California, March 24-28, 2003.
[10] V. Perez-Reale et al, *Triggering Standard Model Higgs processes in the ATLAS experiment*, Proceedings of "Physics at LHC" 2004 conference, Vienna 13-17th of July 2004, Czechoslovak Journal of Physics, Vol. 54 (2004), Suppl. A.